

**Evelyn Eger, Christian A. Kell and Andreas Kleinschmidt**

*J Neurophysiol* 100:2038-2047, 2008. First published Jul 16, 2008; doi:10.1152/jn.90305.2008

**You might find this additional information useful...**

---

This article cites 27 articles, 6 of which you can access free at:

<http://jn.physiology.org/cgi/content/full/100/4/2038#BIBL>

Updated information and services including high-resolution figures, can be found at:

<http://jn.physiology.org/cgi/content/full/100/4/2038>

Additional material and information about *Journal of Neurophysiology* can be found at:

<http://www.the-aps.org/publications/jn>

---

This information is current as of November 27, 2008 .

## Graded Size Sensitivity of Object-Exemplar-Evoked Activity Patterns Within Human LOC Subregions

Evelyn Eger,<sup>1,2,3</sup> Christian A. Kell,<sup>4</sup> and Andreas Kleinschmidt<sup>1,2,3</sup>

<sup>1</sup>*Institut National de la Santé et de la Recherche Médicale, U562, Gif/Yvette, France;* <sup>2</sup>*Commissariat à l'Énergie Atomique, Direction des Sciences du Vivant, Institute d'Imagerie Biomedicale, NeuroSpin, Gif/Yvette, France;* <sup>3</sup>*University Paris-Sud, Orsay, France;* and <sup>4</sup>*Brain Imaging Center, Department of Neurology, University of Frankfurt, Frankfurt, Germany*

Submitted 26 February 2008; accepted in final form 12 July 2008

**Eger E, Kell CA, Kleinschmidt A.** Graded size sensitivity of object-exemplar-evoked activity patterns within human LOC subregions. *J Neurophysiol* 100: 2038–2047, 2008. First published July 16, 2008; doi:10.1152/jn.90305.2008. A central issue for understanding visual object recognition is how the cortical hierarchy represents incoming sensory information and transforms it across successive processing stages. The format of object representation in the human brain has thus far mostly been studied using adaptation paradigms because the neuronal layout of object selectivities was thought to be beyond the resolution of conventional functional MRI (fMRI). Recently, however, multivariate pattern recognition succeeded in discriminating fMRI responses of object-selective cortex to different object exemplars within a given category. Here, we use increased spatial fMRI resolution to explore size sensitivity and tolerance to size change of response patterns evoked by object exemplars across a range of three sizes. Results from Support Vector Classification on responses of the human lateral occipital complex (LOC) show that discrimination of size (for a given object) and discrimination of objects across changes in size depended on the amount of size difference. Even across the largest amount of size change, accuracy for generalization was still significant in LOC, whereas the same comparison was at chance performance in early visual (calcarine) cortex. Analyzing subregions, we further found an anterior-posterior gradient in the degree of size sensitivity and size generalization within the posterior-dorsal and anterior-ventral parts of LOC. These results speak against fully size-invariant representation of object information in human LOC and are hence congruent with findings in monkeys showing object identity and size information in population activity of inferotemporal cortex. Moreover, these results provide evidence for a fine-grained functional heterogeneity within human LOC beyond the commonly used LO/fusiform subdivision.

### INTRODUCTION

Object recognition requires the visual system to overcome ambiguities of the retinal image caused by different viewing conditions. A common view is that when progressing along the hierarchy of the ventral visual stream, neurons gain selectivity to specific objects in parallel with increasing tolerance of changes in for instance object position, distance, and viewing angle (DiCarlo and Cox 2007; Riesenhuber and Poggio 2002). However, the detailed characteristics of neural representations and their transformation across object selective areas remain largely unknown. In monkey inferotemporal (IT) cortex, many individual neurons respond to objects in specific views or sizes with a smaller number generalizing across these transformations (Ito et al. 1995; Logothetis et al. 1995; Lueschow et al.

1994). Conversely, neuronal population signals carry information about object identity (despite changes in position and size) as well as size and position themselves (Hung et al. 2005).

Previous functional imaging research in humans mostly used functional MRI (fMRI) adaptation paradigms, inferring properties of neural representations indirectly by measuring fMRI signal changes associated with repetition of the same stimulus and its variants (see Grill-Spector et al. 2006; for a review). However, studying the neural basis of object representation ideally requires techniques that can distinguish neural responses to individual, and highly similar, objects. Recently, multivariate pattern recognition techniques have been successfully used to exploit the information in fine-scale fMRI activity patterns (see Haynes and Rees 2006; Kriegeskorte and Bandettini 2007; for reviews; Norman et al. 2006). Using such approaches, one of us (Eger et al. 2008) reported discriminability of direct evoked fMRI patterns for within-category exemplars of objects in the human lateral occipital complex (LOC). A key finding in that study was that LOC response patterns permitted to identify object exemplars across changes in size and viewing angle but not to discriminate size and view above chance, unlike findings from monkey neurophysiology (Hung et al. 2005). However, because of low classification accuracy, that study's failure to detect size and view information in human LOC could reflect a floor effect or the small range of size changes used. Given the scale of neuronal clustering of object selectivities, which is  $\sim 500 \mu\text{m}$  in the monkey (Fujita et al. 1992), it is also possible that the spatial resolution of the fMRI acquisition in that study was insufficient.

To enhance decoding capacity, this study therefore used threefold higher MRI resolution and a broader range of sizes in an otherwise similar paradigm. LOC normally shows two confluent but nonetheless clearly discernible foci, a posterior lateral occipital (LO), and a fusiform partition (Grill-Spector 2003; Malach et al. 2002). These regions are usually studied as unities in the object processing literature but to which extent they are homogeneous, or consist of further functional subdivisions, is largely unexplored. In this study, we therefore not only compared lateral occipital and fusiform object-selective subregions but also examined the posterior-anterior distribution of object and size information within these two subregions. We provide evidence for functional heterogeneity within both the LO and fusiform object-selective subregions, with

Address for reprint requests and other correspondence: E. Eger, INSERM U.562, Neuroimagerie Cognitive, CEA/NeuroSpin, Bât 145, Point Courrier 156, F-91191 Gif/Yvette, France (E-mail: evelyn.eger@gmail.com).

The costs of publication of this article were defrayed in part by the payment of page charges. The article must therefore be hereby marked "advertisement" in accordance with 18 U.S.C. Section 1734 solely to indicate this fact.

anterior-posterior differences in size sensitivity and size generalization within regions.

## METHODS

### *Participants and data acquisition*

Twelve healthy volunteers (1 left-handed) with normal or corrected vision (3 men and 9 women; mean age,  $25.4 \pm 3.2$  yr) gave written informed consent. Functional images were acquired at the Brain Imaging Center of Frankfurt University, Frankfurt, Germany, on a 3-T MR system with eight-channel head coil (Siemens Trio, Erlangen, Germany) as T2\*-weighted echo-planar image (EPI) volumes using a sequence optimized by Wibrál et al. (2007). Twenty transverse slices were obtained with a repetition time of 2 s (echo time, 30 ms; flip angle, 70°;  $2 \times 2 \times 2$ -mm voxels; 0.5-mm gap).

### *Stimuli and design*

Object stimuli (4 chairs and 4 teapots) were the same as previously used (Eger et al. 2008). For each object, three sizes were created with size 2 corresponding along each axis to 150% of size 1 and size 3 to 150% of size 2 (or size 2 to 225% of the area of size 1 and size 3 to 225% of the area of size 2). Chair and teapot stimuli were counter-balanced across subjects, thus presenting each subject with a total of 12 experimental conditions (4 exemplars  $\times$  3 sizes). The low-level similarity (measured as Euclidean distance between pairs of pictures) was on average  $94.7 \pm 33.8$  for object comparisons in the same size,  $104.7 \pm 26.7$  for one step of size change, and  $139.6 \pm 23.8$  for two steps of size change of the same object.

### *Experimental protocol and task*

Stimuli were back-projected onto a translucent screen above the subjects' head and viewed via a mirror on the head coil. Pictures subtended  $\sim 3.3$ ,  $\sim 5$ , and  $\sim 7.5^\circ$  of visual angle for the three sizes. Objects were presented in short blocks of four identical (in exemplar and size) pictures each (1-s stimulus, 0.5-s blank), followed by a fixation baseline of 4 s, with pseudo-randomized order of conditions. Each stimulus randomly appeared in a red or green hue, and participants reported the color of each stimulus via keypad. This task was performed in six experimental sessions of 8.2-min length each, encompassing 24 blocks altogether per experimental condition.

An additional scanning session of  $\sim 5$ -min length mapped object-responsive areas for each participant using a standard LOC localizer, comparing pictures of various common objects to mosaic-scrambled versions of the same images ( $20 \times 20$  fragments). Objects and scrambled images were alternated in blocks with 500 ms per picture every 1 s and block length of 12 s (6-s fixation baseline).

### *Image processing and data analysis*

The initial analysis of the imaging data used SPM5 (<http://www.fil.ion.ucl.ac.uk/spm/software/spm5>). After motion correction and normalization to an EPI-template in MNI space, the unsmoothed EPI images were entered into a general linear model, modeling separately the effect of each of the 12 conditions convolved with a standard hemodynamic response function, while accounting for serial autocorrelation with an AR(1) model and removing low-frequency drift terms by a high-pass filter with a cut-off of 128 s. This analysis yielded six independent estimates of fMRI signal change (corresponding to the 6 sessions), which were subsequently used for pattern recognition analysis.

Object responsive voxels were defined as voxels activated in the contrast of objects versus scrambled objects, on unsmoothed data, within a mask of occipito-temporal areas created with WFU-Pickatlas (<http://fmri.wfubmc.edu/cms/software>). The mask comprised inferior

and medial occipital gyrus, inferior and medial temporal gyrus, and fusiform gyrus, in standard stereotactic space. To obtain roughly equivalent numbers of voxels across participants, we adopted participant-specific thresholding, yielding on average  $1,518 \pm 116$  (minimum, 1,348; maximum, 1,688) voxels, at an average  $t$ -value of  $3.5 \pm 0.9$  (average  $P$  value of 0.004, uncorrected).

To assess potential different sensitivity to object exemplar and size in subregions of LOC, we, as others, first divided object-responsive voxels into a posterior-dorsal lateral occipito-temporal (LO) part and an anterior-ventral fusiform (FUS) part (see Grill-Spector 2003). Subdivision in our study was based on anatomical markers in normalized space, using the aforementioned masks from WFU-Pickatlas. Voxels falling into the masks of inferior and medial occipital and temporal gyrus were considered as LO and voxels falling into the masks of fusiform gyrus as FUS. Although this procedure might not capture individual functional anatomy perfectly in each case, it is based on a simple, unbiased, and objective criterion that permits comparison or replication across studies. Using the thresholds mentioned above, this subdivision yielded on average  $1,012 \pm 94$  voxels for LO and  $506 \pm 141$  voxels for FUS across participants [see Fig. 1A for a map of the average location of these regions of interest (ROIs)]. We further partitioned the ensemble of voxels activated in each subject's localizer contrast in posterior-anterior ( $y$ ) direction, resulting in two (and in additional analyses, 4 and 8) subdivisions for LO and FUS. This subdivision did not rely on any further anatomical marker but was done such that voxel numbers were the same for each subdivision in each given subject. For comparative purposes, regions of early visual cortex were defined by a mask covering the calcarine sulcus in MNI space, from WFU-Pickatlas.

Control analyses were performed for ROIs that equated both the number of voxels and the functional signal-to-noise ratio between posterior (LO) and anterior (FUS) parts of LOC. First, the 1,000 most object-selective (objects  $>$  scrambled) voxels were selected within the anatomical masks described above for LO and FUS, respectively. Subsequently, voxels with the highest  $t$ -value for LO and the lowest  $t$ -value for FUS were eliminated in an iterative procedure until the average  $t$ -value was comparable between the two ROIs. An analogous procedure was used to equate the  $t$ -value for all stimuli versus fixation between the two regions. (see Supplemental Fig. 1 for results and details of voxel numbers).<sup>1</sup>

Pattern recognition analysis was used to predict which of two given stimuli was presented on test trials from distributed response patterns within ROIs. The fMRI signal change estimates (parameter estimates) of the  $n$  voxels in a given ROI for each condition and for repeated sessions were extracted. Classification analyses were performed on the mean-corrected pattern across voxels, and for comparison on the mean across voxels, corresponding to univariate (whole ROI) analysis. Linear support vector machines (Christianini and Shawe-Taylor 2000; see Cox and Savoy 2003; Kamitani and Tong 2005; Mourao-Miranda et al. 2005 for examples of application in fMRI; support vector machines: Vapnik 1995) were used in the implementation of Gunn (<http://www.isis.ecs.soton.ac.uk>) with a fixed regularization parameter of  $C = 5$ , performing leave-one-out-classification with sixfold (6 independent sessions) cross-validation. SVM being essentially a method for pair-wise classification, all possible pair-wise comparisons were tested, and accuracy subsequently were averaged for discrimination of object exemplar size across one step or two steps, etc. (chance corresponding to 50%). The pattern classification process is described in more detail in Eger et al. (2008). For all analyses studying prediction accuracy as a function of the number of voxels included, voxels were rank-ordered on the basis of their  $t$ -value for visual stimulation versus baseline (an orthogonal contrast that permits comparing accuracy between comparisons involving objects and sizes with identical voxels included).

<sup>1</sup> The online version of this article contains supplemental data.

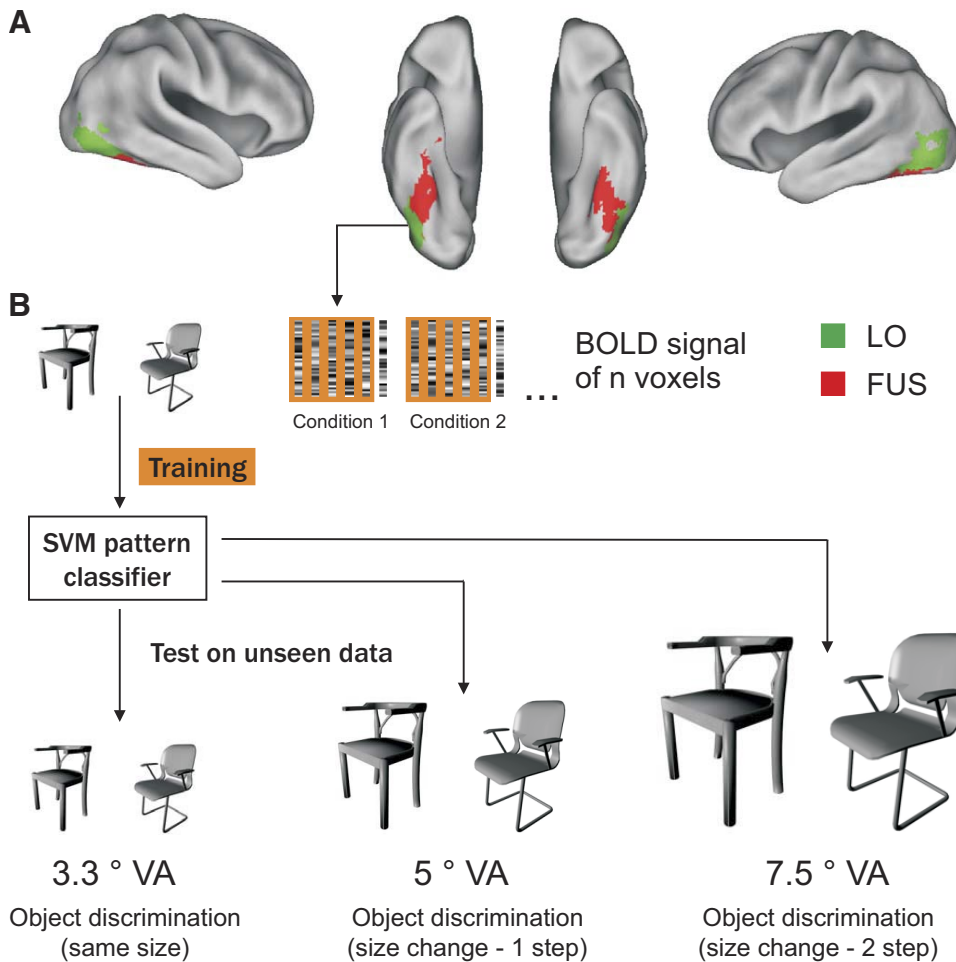


FIG. 1. Analysis procedures. *A*: group map ( $n = 12$ ) of object-responsive areas (defined as responding more to objects than scrambled objects) at  $P < 0.0001$ , uncorrected. For pattern recognition analysis as performed here, this region was defined on a subject-by-subject basis. Shown in green and red are group activations for the posterior-dorsal lateral occipital (LO) and anterior-ventral fusiform (FUS) parts of the lateral occipital complex. The functional MRI (fMRI) signal change across voxels was extracted separately for each session and condition from these regions of interest (ROIs) and entered into pattern recognition analysis (support vector machines) based on leave-one-out prediction with cross-validation. *B*: a linear classifier was trained on data from a given pair of objects and tested on data corresponding to the same size (object discrimination—same image) or a different size (object discrimination—size generalization) for 3 sizes corresponding to 3.3, 5, and 7.5° of visual angle. In an analogous way, discrimination was performed on data corresponding to different sizes of a given object (separated by 1 or 2 steps of size change), where the classifier was subsequently tested on the 2 sizes of the same object or another object (data not shown).

In addition to testing discrimination of object exemplars (with and without size change) and sizes, we estimated the lower and upper bound of the SVM classifier in this data set. The lower bound was estimated by classifying the same objects in the same size and the upper bound by classifying between different objects in different sizes for the largest size change used. Results and more details can be found in Supplemental Fig. 2.

Two indices were used for quantification of size sensitivity and size generalization in comparisons across regions. The size sensitivity index corresponds to the ratio of discrimination of, and generalization of object discrimination across, a given size change ( $SSI = ACC_{size\_discrim}/ACC_{object\_diffsize}$ ) separately for the two steps of size change. The size generalization index was computed as the ratio of generalization of object discrimination across a given size change and object discrimination in the same size ( $SGI = ACC_{object\_diffsize}/ACC_{object\_samesize}$ ). The rationale for the use of these two indices is to give a more complete description of the size sensitivity/size invariance in a given region. Previous work using pattern recognition showed, for example, that early visual cortex can show rather accurate generalization of object discrimination across size change because of low-level stimulus overlap between conditions (Eger et al. 2008). An index that sets into relation size discrimination and (generalization of) object discrimination may therefore help to disambiguate performance based on invariant object representation from that based on low-level stimulus features. Because of their relative nature, both indices used are insensitive to differences in overall classification accuracy across regions that may arise for instance from differences in functional contrast-to-noise and thus be unrelated to the question of interest.

## RESULTS

### Information on object exemplar and size in mean activity and patterns of LOC

First, we analyzed pattern signals from the entire object selective ROI. For discrimination of objects, we tested classification performance in the same size and in a different size (across 1 or 2 steps of size change). We also tested for discrimination of size itself across one or two steps of difference, either in the same object or when training the classifier on two sizes of one object and subsequently testing on another object. Each analysis was conducted for mean activity (across voxels) as well as for selected numbers of voxels of the mean-corrected pattern (see METHODS for details).

Discrimination performance for objects was at or close to chance for average activity across the ROI but increased when selecting voxels on the basis of their overall visual response and turned asymptotic at  $\sim 85\%$  correct performance (for training and test on identical image sizes; Fig. 2A). Classification performance for test on data from the same object, but in a different size, decreased with the degree of size change: one step of size change in test objects yielded only slightly lower performance ( $\sim 80\%$  correct) than for the same size, whereas two steps resulted in clearly reduced but still reliable above chance performance ( $\sim 70\%$  correct). Discrimination of size (for the same object) across one step of size change yielded

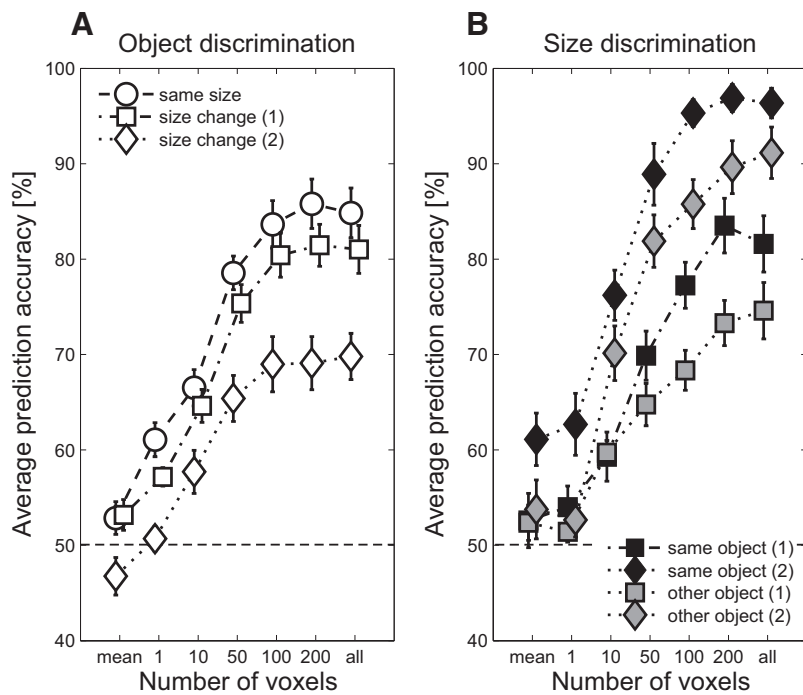


FIG. 2. Pattern recognition results for the entire lateral occipital complex (LOC) region. Discrimination performance (mean across 12 subjects and SE) for object discrimination (A) and size discrimination (B). For the results in A, the classifier was trained on each one of all possible pairs of objects and subsequently tested on the same object pair either in the same size or in a different size (size changes 1 and 2 corresponding to the 2 steps used). For the results in B, the classifier was trained on 2 sizes for a given object (that could differ in 1 or 2 steps of size change) and subsequently tested on those 2 sizes of the same object or all other possible objects. Analysis was conducted for the mean signal across voxels and for increasing numbers of voxels of the mean-corrected pattern shown here for  $\leq 200$  voxels, as well as for all voxels.

slightly lower classification performance than discrimination of different objects in the same size, whereas the same discrimination across two steps of size change resulted in markedly increased classification accuracy of up to  $\sim 95\%$ . When testing the size classifier on another object than the one used for training, classification accuracy were reduced by  $\sim 10\%$  and were relative to performance on the same object. This reduction held for both degrees of size change (1 and 2 steps), but performance always still remained well above chance (Fig. 2B).

Classification accuracy for one step of size change were further analyzed separately for generalization from size 1 to 2 (and vice versa) and generalization from size 2 to 3 (and vice

versa), as well as discrimination of size 1 and 2 and size 2 and 3. These data (Fig. 3) show a small tendency for weaker generalization across the two larger sizes, which, however, did not reach significance in any of the cases. With size discrimination, a similar tendency was observed for better discrimination between the two larger sizes that reached significance in a pairwise *t*-test in a few cases (i.e., for mean activity and 10 and 50 voxels in the case of test on the same object, and for 200 and all voxels in the case of test on a different object). This finding of slightly better discrimination of the larger sizes might be related to the fact that, although the two comparisons involve the same relative size change, this implies a larger

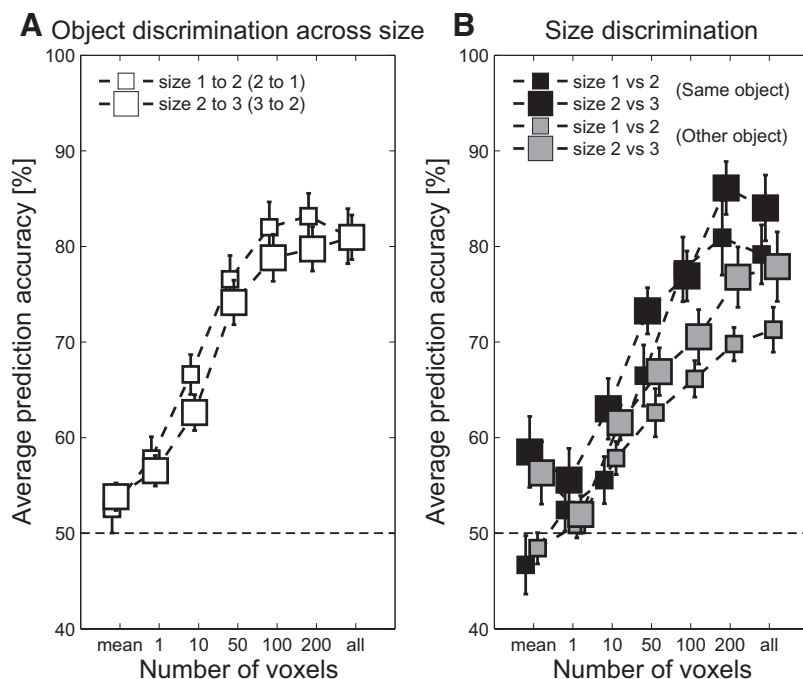


FIG. 3. Pattern recognition results for the entire LOC region. Discrimination performance (mean across 12 subjects and SE) for object discrimination across size change (A) and size discrimination (B). Results are shown separately for the 2 size changes with equivalent (1-step) relative difference: size 1 vs. 2, and size 2 vs. 3. A small tendency for better discrimination of the larger size change in absolute terms is observed.

absolute increase in edge length (and even more area) between the two larger sizes (see Fig. 1).

To summarize, discrimination of object exemplars across changes in image size, as well as discrimination of size itself, depends on the relative amount of size change, and given a large enough size difference, information about size is detectable in LOC with even higher reliability than information about the objects used here.

#### Object and size information in patterns of LOC subregions and early visual cortex

To test for potential regional differences in size invariance of object information, we next assessed information on object exemplar and size separately for subregions of object-selective cortex. First, we examined separately LO and FUS parts of the object-selective cortex.

Results of classification using all voxels in these ROIs without further selection are shown in Fig. 4, *A* and *B*. Apart from a slight overall difference in absolute classification accuracy, which are higher in LO, the two object-selective subregions show a very similar pattern of results. Object discrimination across size change and size discrimination depended on the amount of size change to nearly the same degree. Furthermore, in both regions, discrimination of size across two steps of size change yields classification accuracy superior to those for discrimination of objects.

The results from both object-selective ROIs contrast clearly with findings from early visual (calcarine) cortex (Fig. 4*C*). Although generalization of object discrimination in LOC is above chance, even across the two steps of size change used, the same comparison is at or near chance performance in early visual cortex. This is found even though overall discrimination performance in early visual cortex (nearly 100% correct for size and object in the same size) is higher than in LOC.

Quantification of relative size sensitivity and size generalization in these different regions used two indices taking into account size discrimination, as well as object discrimination across sizes and in the same size (see METHODS; Fig.

4, *D* and *E*). The size sensitivity index (SSI) was higher in early visual cortex than in LOC [LO vs. early visual,  $F(1,11) = 32.6$ ,  $P < 0.001$ ; FUS vs. early visual,  $F(1,11) = 19.6$ ,  $P < 0.001$ ] but comparable between lateral occipital and fusiform object-selective subregions [ $F(1,11) = 0.08$ ]. Accordingly, the size generalization index (SGI) was increased in LOC compared with early visual cortex [LO vs. early visual,  $F(1,11) = 55.6$ ,  $P < 0.001$ ; FUS vs. early visual,  $F(1,11) = 54.4$ ,  $P < 0.001$ ] but not significantly different between LO and FUS [ $F(1,11) = 0.6$ ].

Since at a given identical threshold the fusiform subpart of LO is commonly smaller than the lateral occipital part, the average number of voxels included in our original ROIs was different between the two regions (see METHODS). To test how far this could explain the overall lower discrimination performance observed in the fusiform ROI, we performed control analyses that equated the number of voxels and the functional signal-to-noise ratio between regions (see METHODS for details and Supplemental Fig. 1). Results were nearly identical to the previously described ones, both for equating the mean  $t$ -value for objects versus scrambled (Supplemental Fig. 1, *A* and *B*), and visual versus baseline (Supplemental Fig. 1, *C* and *D*) between the two subregions. This suggests that the overall lower classification performance observed in fusiform compared with lateral occipital cortex is caused by other factors than the number of voxels included or the functional signal-to-noise ratio. Furthermore, the finding of comparable size sensitivity and size generalization indices in the two regions was unchanged in these control analyses.

To summarize, absolute discrimination performance was overall slightly higher in LO than FUS but reliably above chance in both regions. A very similar pattern of classification accuracy across the different comparisons was observed in both of these object-selective regions, resulting in nearly identical estimates of size sensitivity and size generalization indices. Furthermore, size sensitivity indices in both LO and fusiform cortex were decreased compared with early visual cortex, whereas size generalization indices were increased.

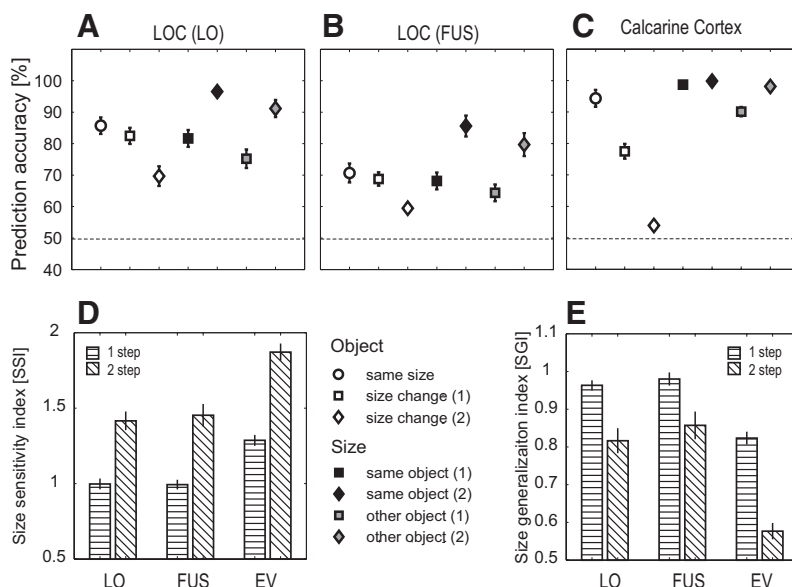


FIG. 4. Pattern recognition results for subregions of LOC. Discrimination performance (mean across 12 subjects and SE) for object and size discrimination for the posterior-dorsal (LO) and anterior-ventral (FUS) subregions of LOC (*A* and *B*). This analysis was performed on the mean-corrected pattern over all voxels in each ROI without further preselection. *C*: results of an analogous analysis performed on data from early visual (calcarine) cortex. *D*: size sensitivity indices were calculated as the ratio of discrimination of size in the same object and object discrimination across size change, for 1 and 2 steps of size change, respectively. *E*: size generalization indices were calculated as the ratio of object discrimination across size change and object discrimination without size change, for 1 and 2 steps of size change. These indices show equivalent size sensitivity and size generalization in LO and fusiform cortex, whereas size sensitivity is decreased in both LOC regions compared with early visual cortex, and size generalization is enhanced.

*Gradient of size sensitivity within LO and fusiform cortex*

Although pattern analyses found equivalent size invariance of responses in the two object-selective subregions when they were tested as a whole, we reasoned that potential differences might exist within each of these regions and might be expressed most likely along the posterior-anterior direction. We therefore subdivided each subject's set of voxels for both LO and FUS into (initially) two equally dimensioned anterior and posterior subsets (see METHODS for details of subpartitioning). The mean average *y* coordinates across subjects of these subdivisions were  $-82.4 \pm 2.9$  for posterior LO,  $-66.9 \pm 3.0$  for anterior LO,  $-64.8 \pm 3.8$  for posterior fusiform, and  $-43.8 \pm 2.7$  for anterior fusiform partitions.

Classification results for all the different comparisons involving discrimination of objects and size within these subdivisions are shown in Fig. 5, *A* and *B*, along with the resulting measures of size sensitivity and size generalization indices (Fig. 5, *E* and *F*). For both the lateral occipital and fusiform regions, discrimination accuracy for sizes relative to objects were reduced in the anterior compared with the posterior subdivisions. This effect is reflected in lower size sensitivity indices for anterior as opposed to posterior subdivisions of both regions. At the same time, the decrease in accuracy for object discrimination across size change was flattened in the anterior compared with posterior parts, resulting in an increase of size generalization indices from posterior to anterior. ANOVAs on both measures were performed with the factors of region (LO/FUS), subdivision (posterior/anterior), and size

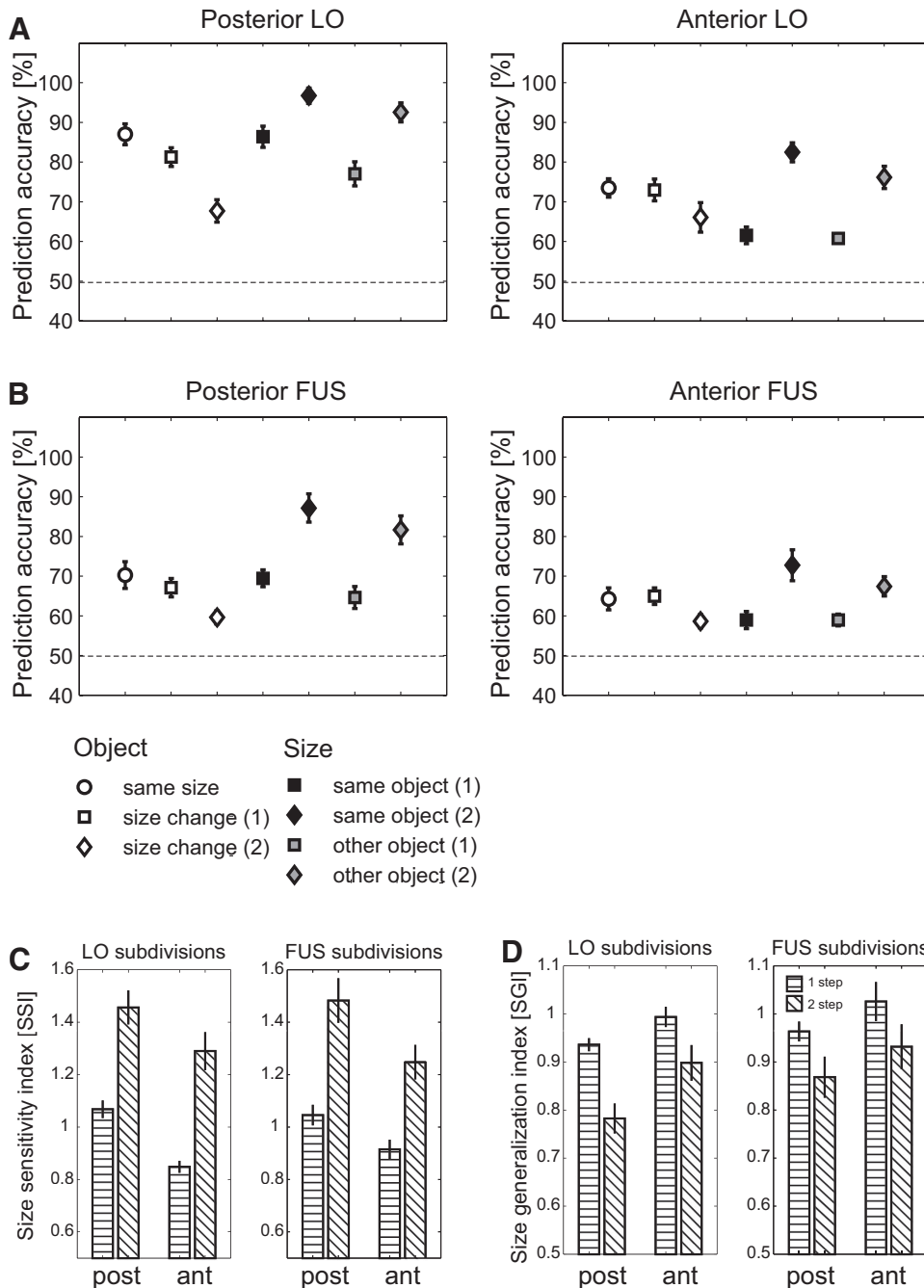


FIG. 5. Pattern recognition results for posterior vs. anterior parts of the LOC subregions LO and FUS. Discrimination performance (mean across 12 subjects and SE) for object and size discrimination (*A* and *B*) performed on the mean-corrected pattern over all voxels in each sub-ROI without further selection. Size sensitivity indices (*C*) and size generalization indices (*D*) show significant main effects in posterior-anterior direction.

change (1 step/2 step). Main effects of size change are highly significant in all cases, as expected (Fig. 5, C and D). The ANOVA on size sensitivity indices also confirmed a significant main effect of subdivision [posterior/anterior;  $F(1,11) = 21.9$ ,  $P < 0.001$ ]. The main effect of region [ $F(1,11) = 0.02$ ], as well as the region by subdivision interaction [ $F(1,11) = 0.01$ ], did not reach significance. When analyzing data from both LO and FUS cortex separately, main effects of subdivision (posterior/anterior) were significant in both LO [ $F(1,11) = 12.9$ ,  $P < 0.01$ ] and FUS [ $F(1,11) = 7.7$ ,  $P < 0.05$ ]. The analogous ANOVA on the size generalization indices equally showed a significant main effect of subdivision [posterior/anterior;  $F(1,11) = 8.6$ ,  $P < 0.05$ ] but not an effect of region [ $F(1,11) = 1.5$ ] or a region by subdivision interaction [ $F(1,11) = 0.2$ ]. When analyzing data from both LO and FUS cortex separately, the main effect of subdivision (posterior/anterior) was significant in LO [ $F(1,11) = 8.8$ ,  $P < 0.05$ ] but failed to reach significance in FUS [ $F(1,11) = 2.2$ ].

Further analyses that were performed with finer partitioning showed that the anterior-posterior difference of size sensitivity in our data was not restricted to the two subdivisions that the data

were divided into initially. The results of analyses using eight subdivisions are shown in Fig. 6. These data show a largely gradual decrease of size sensitivity from posterior to anterior and a somewhat less clear gradual increase in size generalization.

To summarize, when subdividing the voxels within both lateral occipital and fusiform cortex along the posterior-anterior (y) direction, a systematic decrease of size sensitivity and an increase of relative size generalization is observed when progressing from posterior to anterior. This effect is observed despite comparable measures of size sensitivity and generalization when comparing both regions as a whole.

DISCUSSION

This study used multivariate pattern recognition at a spatial resolution that is three times as high as in the wide majority of fMRI studies. We studied size sensitivity and size generalization of human LOC response patterns to object exemplars across a range of three different sizes. We replicated previous results (Eger et al. 2008) by successfully discriminating re-

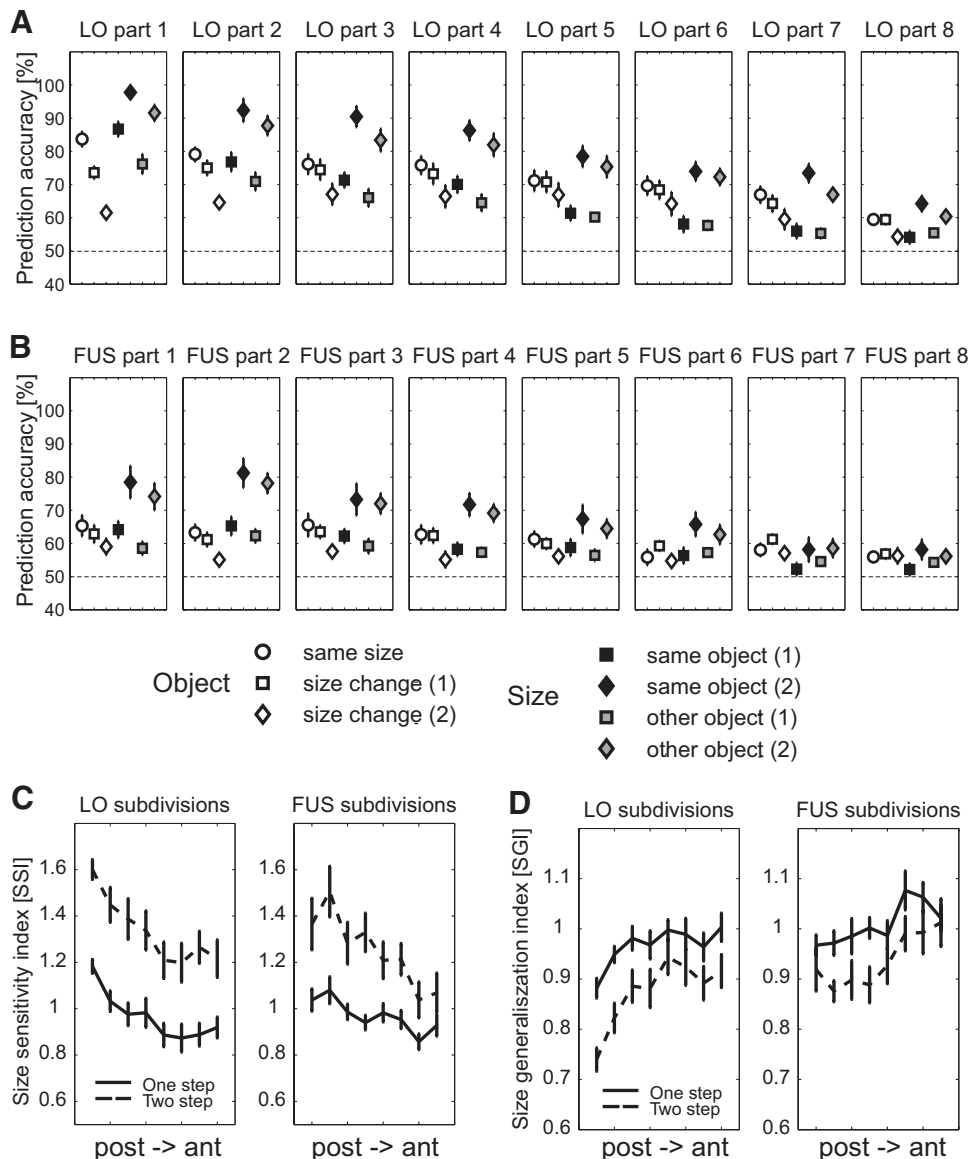


FIG. 6. Pattern recognition results from subdivision of LOC subregions LO and FUS into 8 parts each in posterior-anterior (y) direction. Discrimination performance (mean across 12 subjects and SE) for object and size discrimination (A and B) performed on the mean-corrected pattern over all voxels in each ROI subpart without further selection. Size sensitivity indices (C) show a decrease from posterior to anterior in both LO and FUS, whereas size generalization indices (D) show an increase.

sponse patterns evoked by within-category exemplars of objects. More importantly and in accord with the premises that motivated this study, we found that generalization of classification performance across changes in size was gradual as a function of the relative size change, as was discrimination of size itself. With the object and size settings of our study, sizes could be discriminated at least equally well or even with higher accuracy than different objects for a given size.

These findings extend previous results (Eger et al. 2008), where activity patterns were discriminable above chance in LOC for different objects but not for different sizes. The previous failure to separate responses to different sizes is likely because of the overall low classification accuracy in that study. In the findings presented here, accuracy for size discrimination across one step (corresponding to the same relative difference as used previously) was slightly lower than for object discrimination, but both are well above chance. It is likely that the gain in sensitivity is caused by the increased spatial resolution used in the fMRI acquisition of this study.

These findings agree well with those from electrophysiology in nonhuman primates. Using similar pattern recognition methods, object identity and size information could be read out from multiunit neuronal responses in monkey infero-temporal (IT) cortex (Hung et al. 2005). Thus both modalities converge in indicating that, although object representations in monkey IT cortex and human LOC tolerate size change over a certain range, size information is nevertheless not lost in the population signal. Preservation of size information in IT/LOC signals is likely related to the fact that neurons' receptive fields do not encompass the whole of the visual field. Data from monkey studies suggest receptive field sizes in IT between  $\sim 3$  and  $25^\circ$  (Op de Beeck and Vogels 2000), whereas comparable quantitative data in humans do not exist to our knowledge. Related to this, one recent theoretical model addressing the problem of object recognition across image changes (DiCarlo and Cox 2007) showed that generalization across for example position and size can arise from populations of spatially broadly tuned object-selective neurons. According to that view, invariance at the single neuron level would not be a necessary goal of processing in inferotemporal cortex, but instead neuronal population responses would be able to represent both object identity and location (size, view) information at the same time.

The finding of better discrimination of sizes than object exemplars in our study might nevertheless at first glance seem surprising for high-level visual areas considered as object-selective. In this context, it is important to consider that the low-level dissimilarity of already one step of size change exceeded that from a change in object exemplar in the same size. The finding of higher accuracy for size discrimination across two steps than for objects therefore occurs in the context of an overproportional increase in low-level dissimilarity, whereas for comparable low-level similarity of the size change, this should have resulted in even lower accuracy than in our one-step size change condition. Our data from generalization of object discrimination suggest roughly comparable generalization across size for equivalent relative size changes (size 1 to 2 vs. size 2 to 3), but this effect may not be strictly additive (1 step vs. 2 steps). In addition, for discrimination of size, a tendency for better discrimination for the larger (in absolute terms) of the two comparable relative size changes was observed. This suggests that size discrimination performance may

not be a linear function of the relative size change. However, a more detailed description of the dependence of size discrimination on absolute or relative size changes would require sampling size differences over a still broader range than was possible here.

Our study further compared discrimination performance across and within subregions of human object-responsive cortex. Using the standard subdivision into posterior-dorsal LO and anterior-ventral FUS cortex, we observed overall higher classification accuracy in LO. In previous findings, pattern classification accuracy were also reduced and close to or at chance in FUS cortex (Eger et al. 2008; Williams et al. 2007). However, in contrast to these previous results, the present study had sufficient sensitivity to observe relatively high and reliably above chance discrimination performance not only in LO, but also in the FUS cortex. In this study, we could further rule out the possibility that the difference in overall discrimination accuracy between LO and FUS was caused by different numbers of voxels or differences in the functional signal to noise ratio. It is therefore more likely that this inter-regional difference in classifier performance results from differences between regions in the spatial layout of object selectivities that could lead to more or less detectable effects in the multi-voxel patterns signal.

The two indices that we computed for size sensitivity and size generalization enabled us to compare relative discrimination performance between subregions independent from the overall level of performance that may be subject to nonspecific influences. Size sensitivity and size generalization were found to be equivalent between the posterior-dorsal (LO) and anterior-ventral (FUS) subregions of LOC but markedly different from early visual cortex. Despite the lack of overall difference between posterior-dorsal and anterior-ventral LOC subregions, we observed a systematic decrease of size sensitivity (and increase of size generalization) in pattern signals within both object selective regions when progressing from posterior to anterior. Such a topographic gradient was not reported (or not tested for) in the pattern-based studies in monkey cortex (Hung et al. 2005).

The gradients of size sensitivity (and size generalization) found by us may suggest that, in addition to the enlargement of receptive fields occurring between subsequent stages of early visual cortex, receptive field sizes gradually increase further from posterior to anterior in object-selective visual cortex. Although these regions in human cortex have long been thought of as largely nonretinotopic (Malach et al. 2002; Tootell et al. 1996), recent data support the existence of several retinotopic subdivisions in posterior (LO) and anterior-ventral (FUS) object-selective cortex (Larsson and Heeger 2006; Wandell et al. 2007). The analysis of retinotopic properties in lateral occipital cortex conducted by Larsson and Heeger (2006) showed two subregions (LO1 and LO2), where retinotopy measured in terms of voxel response fields was slightly weaker in the more anterior LO2 than the more posterior LO1. This finding was interpreted to reflect larger receptive fields in the more anterior region. It should be pointed out that, in our study, the definition of ROIs was based on object selectivity but not on retinotopic criteria. In addition to the retinotopic subdivisions LO1 and LO2, the posterior-dorsal (LO) area in our study may also have included voxels from, for example, V3A/B or V5, which can show slightly enhanced responses to objects

compared with scrambled pictures (Grill-Spector and Malach 2004; Larsson and Heeger 2006). Nonetheless, our finding of the size sensitivity gradient in the whole of LOC also points to increasingly larger receptive fields of object-selective neurons when progressing from posterior to anterior, not only within LO but also in the FUS cortex. Across both regions, we observed an apparently smooth gradient of size sensitivity (and generalization) without clear evidence for discontinuity from boundaries, and further studies will have to clarify how potential continuous or discontinuous changes of size sensitivity map onto regions defined by other functional criteria as, for example, retinotopy.

Previous studies of size invariance in LOC responses using fMRI adaptation or priming (Grill-Spector et al. 1999; Sawamura et al. 2005; Vuilleumier et al. 2002) reported some degree of generalization of the adaptation effect for objects across size change. These results are consistent with our findings but we are not aware of fMRI adaptation data for size discrimination that would be comparable to the pattern recognition results reported here. Furthermore, surprisingly, none of the previous studies have investigated size invariance parametrically as a function of the amount of size change. Instead, the range of sizes used was always collapsed into a single condition. Our study therefore makes a first step toward investigating the “size tuning” of neural populations in human visual object processing areas.

Adaptation studies have focused on reporting generalization of the repetition-related fMRI signal decrease across size change. More specifically, in one study using a priming paradigm with seconds or minutes between intervening stimuli, virtually complete generalization of repetition-related decreases in the BOLD signal across changes in object size was observed in all occipito-temporal areas studied, but that study used only moderate changes in size (Vuilleumier et al. 2002). Other studies suggested regional differences with some generalization across size in the anterior-ventral (fusiform) but less in the posterior-dorsal (LO) subregion (Grill-Spector et al. 1999; Sawamura et al. 2005). That latter study (Sawamura et al. 2005) also reported a gradual progress of size generalization of the adaptation effect along axes from posterior to anterior within the LOC. Interestingly, however, these results differ from our findings in that this gradual progress was associated with an overall higher size invariance index (and overall more adaptation) in the fusiform region compared with LO. This observation hence contrasts with the findings obtained by the pattern analysis approach, where the size generalization index was not overall significantly enhanced when progressing from LO to FUS cortex. Instead, we observed main effects in the form of an anterior-posterior gradient for size sensitivity and generalization when comparing posterior and anterior parts of both LO and FUS cortex, to the extent that size sensitivity was lower in the anterior subdivision of LO than the posterior subdivision of FUS cortex, although the former was located, on average, slightly more posterior than the latter. Our data do therefore not endorse a sequential, hierarchical relation between posterior LO and ventral temporal/FUS cortex, as often assumed (Grill-Spector 2003; Malach et al. 2002). Instead, our findings suggest a parallel progression of response properties within each of these areas, at least as far as size invariance is considered.

In summary, the findings reported here show that the performance of pattern recognition techniques can benefit from an increase of the fMRI resolution and that this approach can give neurophysiologically plausible insights into mechanisms of object representation. We found that, for a large enough size difference, multivoxel-evoked fMRI activity patterns in human LOC show independent information discriminating object exemplars and size. Tolerance of object discrimination performance for size change is not complete but depends on the relative size difference. Relative size invariance and size generalization were equivalent between the posterior-dorsal (LO) and anterior-ventral (FUS) subregions of LOC, but size sensitivity decreased and size generalization increased from posterior to anterior within both areas. This observation could imply two separate hierarchies of processing in these regions of object selective cortex. Future research regarding the relation to other response properties and mechanisms of invariance should also seek to characterize topographical variations within these regions, instead of considering them as homogenous functional units.

#### ACKNOWLEDGMENTS

We thank the Brain Imaging Center of the University of Frankfurt for use of its imaging facilities.

#### GRANTS

This work was supported by the Volkswagen Foundation.

#### REFERENCES

- Christianini N, Shawe-Taylor J.** *An Introduction to Support Vector Machines and Other Kernel-Based Learning Methods.* Cambridge University Press: Cambridge, 2000.
- Cox D, Savoy R.** Functional magnetic resonance imaging (fMRI) “brain reading”: detecting and classifying distributed patterns of fMRI activity in human visual cortex. *Neuroimage* 19: 261–270, 2003.
- DiCarlo JJ, Cox DD.** Untangling invariant object recognition. *Trends Cogn Sci* 11: 333–341, 2007.
- Eger E, Ashburner J, Haynes J-D, Dolan RJ, Rees G.** fMRI activity patterns in human LOC carry information about object exemplars within category. *J Cogn Neurosci* 20: 356–370, 2008.
- Fujita I, Tanaka K, Ito M, Cheng K.** Columns for visual features in monkey inferotemporal cortex. *Nature* 26: 301–302, 1992.
- Grill-Spector K.** The neural basis of object perception. *Curr Opin Neurobiol* 13: 159–166, 2003.
- Grill-Spector K, Henson R, Martin A.** Repetition and the brain: neural models of stimulus-specific effects. *Trends Cogn Sci* 10: 14–23, 2006.
- Grill-Spector K, Kushnir T, Edelman S, Avidan G, Itzhak Y, Malach R.** Differential processing of objects under various viewing conditions in the human lateral occipital complex. *Neuron* 24: 187–203, 1999.
- Grill-Spector K, Malach R.** The human visual cortex. *Annu Rev Neurosci* 27: 649–677, 2004.
- Haynes J-D, Rees G.** Decoding mental states from brain activity in humans. *Nat Rev Neurosci* 7: 523–534, 2006.
- Hung C, Kreiman G, Tomaso P, DiCarlo JJ.** Fast readout of object identity from macaque inferior temporal cortex. *Science* 310: 863–866, 2005.
- Ito M, Sawamura H, Fujita I, Tanaka K.** Size and position invariance of neuronal responses in monkey inferotemporal cortex. *J Neurophysiol* 73: 218–226, 1995.
- Kamitani Y, Tong F.** Decoding the visual and subjective contents of the human brain. *Nat Neurosci* 8: 670–685, 2005.
- Kriegeskorte N, Bandettini B.** Analyzing for information, not activation, to exploit high-resolution fMRI. *Neuroimage* 38: 649–662, 2007.
- Larsson J, Heeger DJ.** Two retinotopic visual areas in human lateral occipital cortex. *J Neurosci* 26: 13128–13142, 2006.
- Logothetis NK, Pauls J, Poggio T.** Shape representation in the inferior temporal cortex of monkeys. *Curr Biol* 5: 552–563, 1995.
- Lueschow A, Miller EK, Desimone R.** Inferior temporal mechanisms for invariant object recognition. *Cereb Cortex* 4: 523–531, 1994.

- Malach R, Levy I, Hasson U.** The topography of high-order human object areas. *Trends Cogn Sci* 6: 176–183, 2002.
- Mourao-Miranda J, Bokde AL, Born C, Hampel H, Stetter M.** Classifying brain states and determining the discriminating activation patterns: support vector machine on functional MRI data. *Neuroimage* 28: 980–995, 2005.
- Norman KA, Polyn SM, Detre GJ, Haxby JV.** Beyond mind reading: multi-voxel pattern analysis of fMRI data. *Trends Cogn Sci* 10: 424–430, 2006.
- Op de Beeck H, Vogels R.** Spatial sensitivity of macaque inferior temporal neurons. *J Comp Neurol* 426: 505–518, 2000.
- Riesenhuber M, Poggio T.** Neural mechanisms of object recognition. *Curr Opin Neurobiol* 12: 162–168, 2002.
- Sawamura H, Georgieva S, Vogels R, Vanduffel W, Orban GA.** Using functional magnetic resonance imaging to assess adaptation and size invariance of shape processing by humans and monkeys. *J Neurosci* 25: 4294–4306, 2005.
- Tootell RBH, Dale AM, Sereno MI, Malach R.** New images from human visual cortex. *Trends Neurosci* 19: 481–489, 1996.
- Vapnik V.** *The Nature of Statistical Learning Theory*. Berlin: Springer Verlag, 1995.
- Vuilleumier P, Henson RN, Driver J, Dolan RJ.** Multiple levels of visual object constancy revealed by event-related fMRI of repetition priming. *Nat Neurosci* 5: 491–495, 2002.
- Wandell BA, Dumoulin SO, Brewer A.** Visual field maps in human cortex. *Neuron* 56: 366–382, 2007.
- Wibral M, Muckli L, Melnikovic K, Scheller B, Alink A, Singer W, Munk MH.** Time-dependent effects of hyperoxia on the BOLD fMRI signal in primate visual cortex and LGN. *Neuroimage* 35: 1044–1063, 2007.
- Williams MA, Dang S, Kanwisher N.** Only some spatial patterns of fMRI response are read out in task performance. *Nat Neurosci* 10: 685–686, 2007.